Published in Journal of Hydrology 202, issue 1-4, 244-262, 1997
which should be used for any reference to this work

Numerical versus statistical modelling of natural response of a karst hydrogeological system

Laurent Eisenlohr[a,*], Mahmoud Bouzelboudjen[a], László Király[a], Yvan Rossier[b]

[a]*University of Neuchâtel, Institute of Geology, Center of Hydrogeology, Emile Argand 11, CH-2007 Neuchâtel, Switzerland*
[b]*A. T. E., 17 rue du Périgord, F-69330 Meyzieu, France*

Abstract

Structural and hydrodynamic characteristics of karst aquifers are mostly deduced from studies of global responses of karst springs (hydrographs, chemical or isotopic composition). In this case, global response is often used to make inferences with respect to infiltration and ground water flow processes as well as on the hydrodynamic parameters. Obviously, the direct verification of these inferences is very difficult. We have used an indirect method of verification, introducing well defined theoretical karst structures into a finite element model and then analysing the simulated global response according to the currently accepted interpretation schemes. As we know what we are introducing into the numeric model, the consistency of the interpretation may be checked immediately. The results obtained in the hydrogeological study of two karst basins in the Swiss Jura and from 2-D and 3-D numerical simulations show the difficulty of finding structural parameters and hydrodynamic behaviour from statistical methods alone, i.e. correlation analyses discharge–discharge and precipitation–discharge. In effect, our first results show that the form of the correlograms depends on several factors besides the structure of the karst aquifer: (i) on the form of the floods, in other words the contrast between quick flow and base flow, (ii) on the frequency of hydrological events during the period analysed and (iii) on the type of infiltration processes, in other words the ratio of diffuse infiltration to concentrated infiltration. Obviously, the variability of a karst hydrograph is a result of a combination of these factors. Distinction between them is not always possible on hydrographs, and therefore on correlations (discharge–discharge and precipitation–discharge).

Keywords: Karst hydrogeology; Spring hydrographs; Statistical explanation; Numerical simulations; Structure of karst aquifers

* Corresponding author. Fax: 00494215985299.

1. Introduction

The karst aquifer is represented by interconnected karst conduits with a high hydraulic conductivity, and high flow velocities. The karst network is immersed in a low hydraulic conductivity medium with slow flow velocities, and is connected to a main exsurgence, the karst spring. These aquifers are characterized by a heterogeneous and discontinuous porosity and large spatial variability of hydraulic parameters such as porosity, storage coefficient and hydraulic conductivity (e.g. Schoeller, 1967; Király, 1975; Atkinsson, 1977). According to Király et al. (1995), the duality of karst aquifers is a direct consequence of this structure and can be reduced to three factors: (i) duality of the infiltration processes (diffuse or slow infiltration into the low hydraulic conductivity volume and concentrated or rapid infiltration into the channel network), (ii) duality of the ground water flow field (low flow velocities in the fractured volume and high flow velocities in the channel network) and (iii) duality of the discharge conditions (diffuse seepage from the low hydraulic conductivity volume and concentrated discharge from the channel network at the karst spring). It is because of this major heterogeneity that specific methods for karst aquifer study are used. These inherent complexities have led to the use of global responses for the characterization of physical aspects of karst aquifers and thus its hydrodynamical behaviour. In most cases, the inferences are based on the difference response separation method or on the analysis of transfer functions between input and output, i.e. the karst aquifer is considered to be a black-box. Bonacci (1987, 1993), Soulios (1991) analysed directly the form of the whole discharge flow recession, which is influenced by the size and the hydrodynamical characteristics of a karst system. Other authors used the hydrograph component separation with different models to obtain some information about the behaviour of the aquifer (e.g. Forkasiewicz and Paloc, 1967; Drogue, 1972; Mangin, 1975; Bonacci, 1993; Padilla et al., 1994). Other studies employing time series analysis in karst hydrology include the works of Knisel (1972), Brown (1973), Ozis and Keloglu (1976), Dreiss (1982), Jakeman et al. (1984) and Mangin (1984). These authors have chosen to investigate karst aquifers on the basis of the whole hydrograph with statistical methods (i.e. the analysis of transfer functions between input, rainfall and output, spring hydrograph, obtained by black-box or gray-box models). A summary of methods of quantitative karst aquifer studies is given by Ford and Williams (1989) and Kresic (1993). Király and Morel (1976) and more recently Eisenlohr et al. (1997) have shown that some interpretations from hydrograph separation give non-unequivoqual results for studied karst aquifers.

The aim of this paper is to use numerical simulation of ground water flows to test the sensitivity of some statistical methods in ground water flow interpretation, i.e. auto-correlation discharge–discharge and cross-correlation rainfall–discharge.

2. Materials and methods

The basic principle of the statistical methods that we wish to test is to treat the karst aquifer as a filter that lets the entry signal information more or less pass. The method uses analysis and compares entry signals (rainfall) and output signals (hydrograph). The

information of the signals can be treated individually (auto-correlation analysis) or by comparison to one another (cross-correlation analysis). With these statistical methods the karst system includes the soil cover, non-karst terrains, the unsaturated part of the aquifer and the saturated zone connected to the principal output, the karst spring.

2.1. Statistical interpretation of the karst hydrograph

In this method, the analysed object is represented by the entire spring flow hydrograph and the corresponding precipitations extending from a few months to several years. The hydrograph is transformed into a discretized time series of N terms $(x_1 \ldots x_i \ldots x_N)$ for which we calculate m auto-correlation coefficients $(r_0 \ldots r_k \ldots r_m)$. It is advised to take $m = N/3$ (Mangin, 1984) or $m = N/2$ (Box and Jenkins, 1974), but other values may be used, for example $m = 2N/3$. The auto-correlation coefficients are given by:

$$r_k = \frac{\sum (x_i - \bar{x})(x_{i+k} - \bar{x})}{\sum (x_i - \bar{x})^2} \tag{1}$$

where $\bar{x}$ is the arithmetic mean of the X_i values and $k = 0,\ldots,m$. The choice of t_0, the time after which the record is analysed, influences the results (Mangin, 1984). In this case, t_0 has been systematically taken as the beginning of a hydrological cycle or flood, and in all cases at the end of a recession period.

The graph of the r_k values is the correlogram (discharge–discharge) and its shape gives information about the memory effect, the karstification and the ground water flow reserves of the karst aquifer (e.g. Mangin, 1984; Padilla and Pulido-Bosch, 1995). The number of days required for the correlogram to reach values less than or equal to $r_k = 0.2$ gives this information: the faster the drop in the auto-correlation function the weaker the ground water flow reserves in an aquifer and hence an active karst network. Inversely, a strong memory effect will convert a strong discharge into a major stocking of the ground water flow reserves of an aquifer. In a analysis of rainfall and spring discharge data using auto-correlation and spectral analysis, Mangin (1984) added further depth to his interpretation of the Pyreneean karst aquifers. The contrasting reactions of three systems (Aliou, Baget and Fontestorbes) to recharge show that the speed of decline of the three correlogrammes is different: most rapid for Aliou and much more even and gradual for Fontestorbes. The memory effect can thus be gauged to be very great in the Fontestorbes system, but short in the case of Aliou. Mangin (1984) interprets this memory as a reflection of storage in the system at the time of recharge, undrained reserves being considerable in the Fontestorbes basin but slight in the case of Aliou. The cross-correlation between rainfall and spring discharge gives an idea about the impulsive response of the karst system, as well as about the quality of drainage and the ground water flow reserves of the aquifer. The results of these statistical analysis equally allow a classification of karst aquifers between two extreme case: (i) initial state of a poorly drained aquifer with large ground water flow reserves and (ii) final state of a well-developed and connected karst network causing maximum drainage of low permeability volumes of the aquifer and thus leaving low ground water flow reserves (see e.g. Mangin, 1984; Padilla and Pulido-Bosch, 1995).

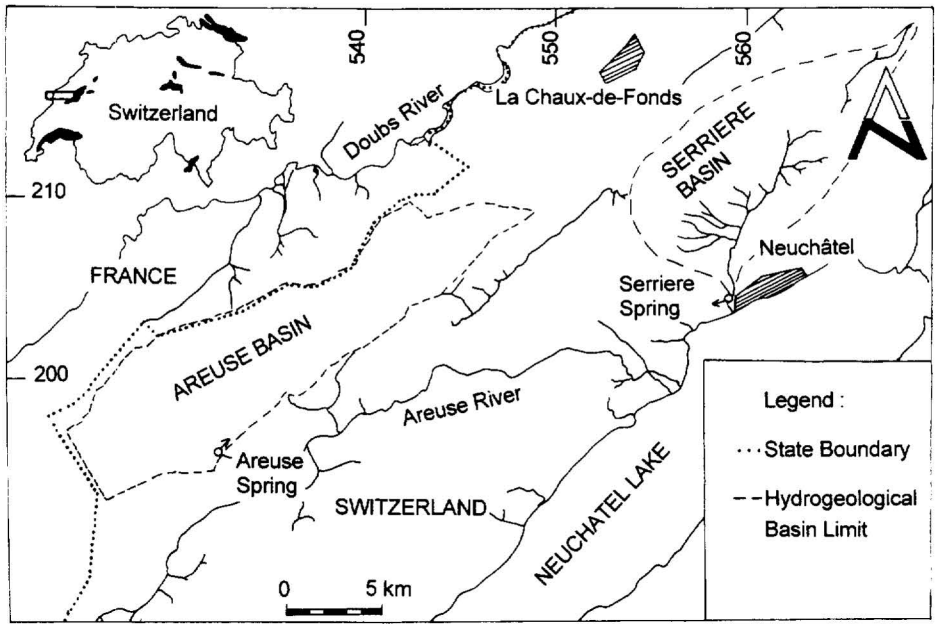

Fig. 1. Location of the catchment area of the Areuse Spring and the Serrière Spring (Canton of Neuchâtel, Switzerland).

3. Application of auto-correlation (discharge–discharge) to two Swiss karst aquifers

The correlatory analysis (discharge–discharge) have been applied to two karst aquifers of the Swiss Jura for an 8 year period. These aquifers are situated in the western Swiss Jura (47° latitude, 6° longitude) (Fig. 1). The Areuse spring drains the ground waters of two synclines with a catchment area of 130 km^2. The Serrière spring drains the ground water of one syncline with a catchment of 80 km^2. The limits of the aquifers are relatively sure,

Table 1
Hydrogeological characteristics for the Areuse and Serrière aquifers

	Areuse Spring	Serrière Spring
Catchment area (km^2)	130	88
Mean altitude of the basin (m)	1115	1060
Main aquifer	Malm	Malm
Mean annual rainfalls (mm)	1520	1350
Outflow deficit (mm)	330	440
Average discharge ($m^3 s^{-1}$)	4.9	2.5
Min. discharge ($m^3 s^{-1}$)	0.3	0.2
Max. discharge ($m^3 s^{-1}$)	51	11
Hydraulic conductivity measured ($m s^{-1}$)	1×10^{-6}–5×10^{-7}	2×10^{-7}–5×10^{-7}
Porosity measured (%)	4.5	4.5
Ground water flow reserves ($10^6 m^3$)	38 (over 10 years)	14 (over 5 years)

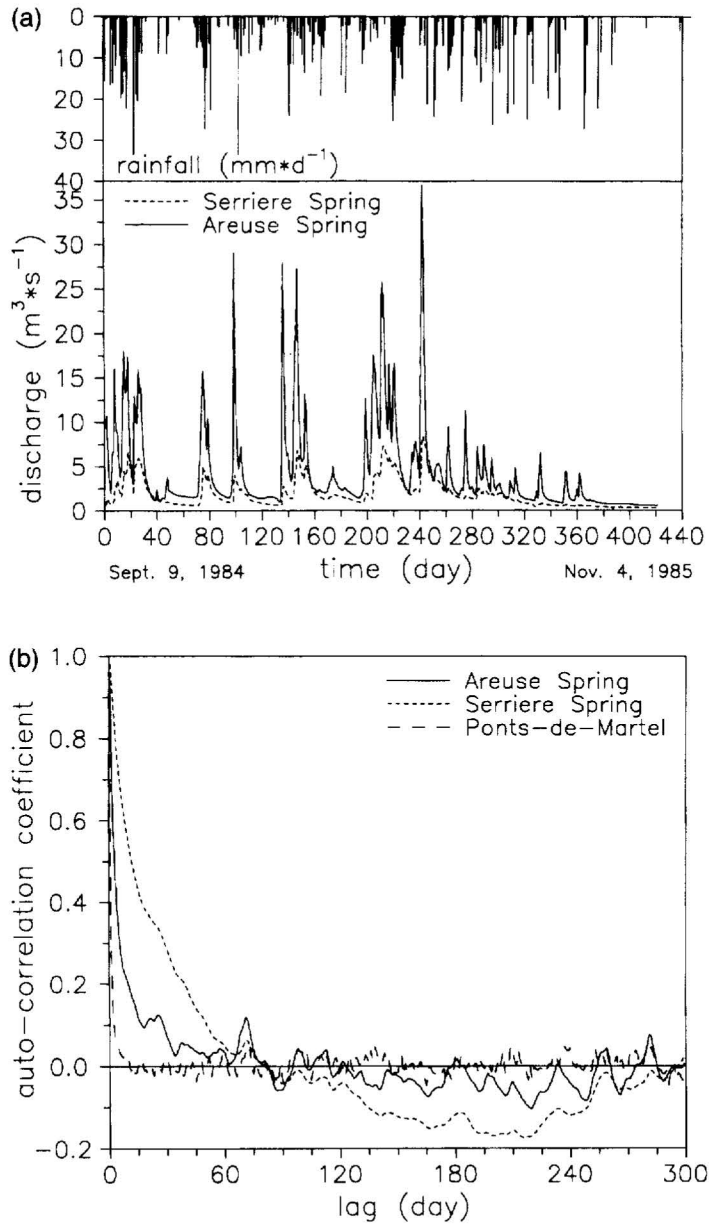

Fig. 2. (a) Hydrographs for the Areuse (——) and Serrière (- - -) Springs for the hydrological cycle 1984–1985. The average daily discharges are obtained from the federal limnimetric stations (canton of Neuchâtel, Switzerland). Daily rainfall for the same period at the climatic station of Ponts-de-Martels (canton of Neuchâtel). (b) Auto-correlations (discharge–discharge) of the Areuse and Serrière Springs for 8 hydrological years (daily values, 1982–1989), m = 400; auto-correlations (precipitation–precipitation) at the Ponts-de-Martels station (daily values, 1982–1989), m = 400.

based on lithological, structural, and geomorphological elements and numerous tracer tests (Király, 1973). The aquifers are in Jurassic limestone, (350 m of Malm), underlain by the quasi-impermeable marls (200 m of Argovien). The Areuse and Serrière basins are separated by the Noiraigue basin, which is 4–6 km wide. Table 1 groups some of the hydrogeological characteristics of these two basins. This information has been taken from the works of Tripet (1973), Mathey (1976) and Burger (1992).

Fig. 2(a) shows that the general forms of the observed hydrographs are comparable. The two basins are subjected to the same climatic regime. The discharge rates of the Areuse Karst Spring are more than four times larger than those of the Serrière Karst Spring. After the peak flood, the decrease in discharges is more rapid for the Areuse Spring. After this fast fall (quick flow), the discharge fall off more steadily (base flow). The contrast between this sharp drop and the stable recession period is less pronounced for the karst spring of the Serrière. Drogue (1972) and Király and Morel (1976) have shown that this contrast beetwen quick and base flow is a feature of karstic aquifers.

Fig. 2(b) shows that the Areuse correlogram drops more quickly than that for the Serrière. The auto-correlation function reaches the $r_k = 0.2$ level after $k = 9$ days for the Areuse and $k = 27$ days for the Serrière. Statistical explanation indicates that the basin of the Areuse spring alters the entry signal very little. The correlogram falls quickly and oscillates around a value of $r_k = 0$ as for the precipitation correlogram. This interpretation indicates that the Areuse basin has smaller ground water flow reserves than those of the Serrière and a larger drainage network. These qualitative interpretations do not match knowledge of field hydrogeology (Tripet, 1973; Mathey, 1976; Burger, 1992) (Table 1). The ground water flow reserves of the Areuse are effectively a factor of two larger than at the Serrière basin. Furthermore, many tracer tests carried out in these two basins have shown high flow velocities which are typical of high permeability zones (Burger, 1992).

In order to study the influence of the forms of the karst spring hydrograph, (see e.g. Király and Morel, 1976; Ford and Williams, 1989; Eisenlohr, 1995; Eisenlohr et al., 1997) on statistical analysis, finite element numerical simulation of ground water flows has been used (Király, 1985, 1988; Király et al., 1995). Four theoretical karst basins have been constructed (Figs. 3–5, and 7). The simulated hydrographs have been analysed by statistical methods: auto-correlation analysis discharge–discharge and cross-correlation recharge–discharge. The consistency of the interpretations of the correlation analyses can be immediately checked as we know the hydrogeological parameters used in the four models K and S_s and the structure of the drainage system. The aim is to show the influence of several parameters in the form of simulated hydrographs on the correlograms and thus to restrict interpretations.

4. Description of computer codes

The computer codes FEN1 and FEN2 have been derived from the computer code FEM301 (Király, 1985), which was previously developed at the Center of Hydrogeology of Neuchâtel and submitted to several rigorous verification tests under the international HYDROCOIN project (O.E.C.D., 1988). FEN1 and FEN2 simulate steady state or transient, 1-D, 2-D or 3-D saturated ground water flow by the finite element method. The

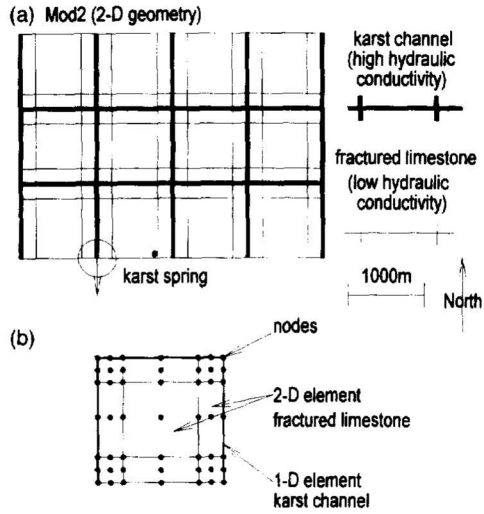

Fig. 3. (a) Finite element network for the variant Mod2. The thin lines represent the boundaries of quadratic finite elements. The thickness of the theoretical aquifer is 50 m, (b) Discretisation of fractured limestone volume.

programs allow for the incorporation of 1-D, 2-D or 3-D linear or quadratic elements within a three dimensional network and are particularly well suited for analysing regional ground water flow systems in highly heterogeneous geologic media (e.g. fractured or karst aquifers). The saturated, constant density, transient ground water flow is represented by the equation (Bear, 1979; de Marsily, 1986)

$$S_s \frac{\partial h}{\partial t} + div(-[K]\cdot \vec{grad}\ h) + Q = 0 \tag{2}$$

where S_s is the specific storage (m^{-1}), K is the hydraulic conductivity tensor ($m\ s^{-1}$), h is

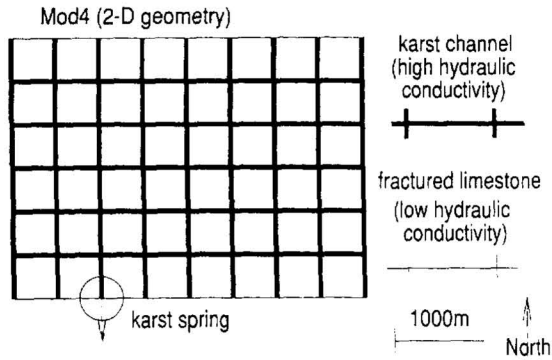

Fig. 4. Finite element network for the variant Mod4. The thin lines represent the boundaries of quadratic finite elements. The thickness of theoretical aquifer is 50 m.

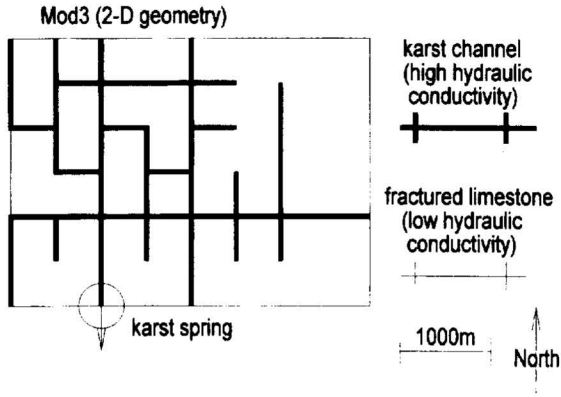

Fig. 5. Finite element network for the variant Mod3. The thin lines represent the boundaries of quadratic finite elements. The thickness of theoretical aquifer is 50 m.

the hydraulic head (m) and Q represents the general source term (infiltration, well discharge). The finite elements formulation of the governing partial equations is done by the Galerkin method, yielding a set of linear equations. Assembling and solving of the system of linear equations is based on the frontal elimination technique of Irons (1970), which is a particularly useful modification of the Gauss elimination procedure. The frontal method is very efficient for very large 3-D problems and allows the modeller to rapidly introduce changes in the geometry of the model. The original code FEM301 and the frontal method are described in detail by Király (1985). The time dependent problem is solved in FEN2 by using the robust Crank-Nicholson implicit time-stepping scheme. In this paper, the high hydraulic

Table 2
Hydrogeological parameters used for the models, (1) epikarst 2-D, (2) epikarst with 261 nodes

	Mod1	Mod2	Mod3	Mod4
Catchment area (km^2)	6	12	12	12
Thickness of aquifer (m)	500	50	50	50
Hydraulic conductivity:				
1-D element ($m\ s^{-1}$)	100	10	10	10
2-D element ($m\ s^{-1}$)	1×10^{-2}(1)	1×10^{-6}	1×10^{-6}	1×10^{-6}
3-D element ($m\ s^{-1}$)	5×10^{-6}	—	—	—
Storage coefficient:				
1-D element	5×10^{-3}	5×10^{-2}	5×10^{-2}	5×10^{-2}
2-D element	—	5×10^{-3}	5×10^{-3}	5×10^{-3}
3-D element	1×10^{-5}	—	—	—
Number of nodes	1428 (2)	1617	1617	1617
Number of elements	232	648	648	648
1-D element	56	264	264	264
2-D element	60 (1)	384	384	384
3-D element	116	—	—	—
Concentrated infiltration injected into 1-D elements (%)	(0,50,100)	20	20	20

conductivity channel network is simulated by 1-D quadratic line elements, which are immersed between 2-D and/or 3-D quadratic elements representing the low hydraulic conductivity fractured limestone volumes (Figs. 3, 4, 5 and 7). Table 2 shows the model characteristics and parameters used in the numerical simulation of ground water flow in the four basins.

The discretisation of the models in finite element is too coarse. However the obtained results seem quite acceptable, although a finer discretization would have been preferable (Király et al., 1995). The hydraulic conductivities K are realistic: from 1×10^{-6} to 5×10^{-6} m s^{-1} for the low hydraulic conductivity fracturated volumes (2-D and 3-D elements) and from 10 to 100 m s^{-1} for the high hydraulic conductivity karst channels (1-D element). Linear Darcy's law is used through the models for both the channel network and the low hydraulic conductivity fractured volume. The specific storage coefficients S_s are kept artificially low in order to accelerate the evolution of the simulated hydraulic head and flow field (Király et al., 1995). In the channel network the values of S_s introduced in the 2-D models are ten times higher than in the lower hydraulic conductivity fractured volumes and 500 in the 3-D model. Finally, it must be emphasized that in both models we have used a very simplified karst channel network. In real systems the karst network is hierarchically organized, with lower and higher order branches having lower and higher hydraulic conductivity values. In the models described above (Table 2) all branches of the karst network are the same order of magnitude and have the same hydraulic conductivity. Despite these deliberate simplifications, the form of the simulated hydrographs is representative of a flood observed at the karst spring (compare Figs 2(a) and 10(a)).

5. Results of the numerical simulations of ground water flows in a karst aquifer

5.1. 2-D numerical simulation of flood hydrograph

We have compared the hydrodynamic responses of the different models, Mod2, Mod3 and Mod4, for a variable recharge lasting 24 hr. The recharge is triangular, going from 0 to a maximum of 3×10^{-7} m^3 s^{-1} m^{-2} in 12 hr (Fig. 6(a)). In the theoretical karst aquifer, the ground water levels and the spring discharges are calculated at each time step ($\Delta t = 1$ hr). The model aquifers are rectangular (4×3 km). Karst conduits leading to the spring are distributed within the fractured rock volume. Throughout the simulation, we can distinguish very slow flows, which correspond to slow velocities in the fractured volume and rapid flows in the karst network. Recharge creates a steady rise in velocity and at each confluence, we see a sharp increase in the flow velocity.

Fig. 6(a) shows the simulated responses of the three basins over a period of 1200 hr. Two main characteristics come out of this figure: (i) the model responses Mod2 and Mod3 are similar despite the differing karst network geometries, (ii) the response of Mod4, whose karst network density is higher is different from that of Mod2 and Mod3. The high amplitude of the flood as well as the form of the recession curve (see discharge from 0 to 250 hr and from 500 to 1200 hr) is characteristic of a well drained aquifer with a dense karst network. At the end of the simulation, the state of the karts ground water in the fractured limestone volumes of low permeability shows that the ground water flow

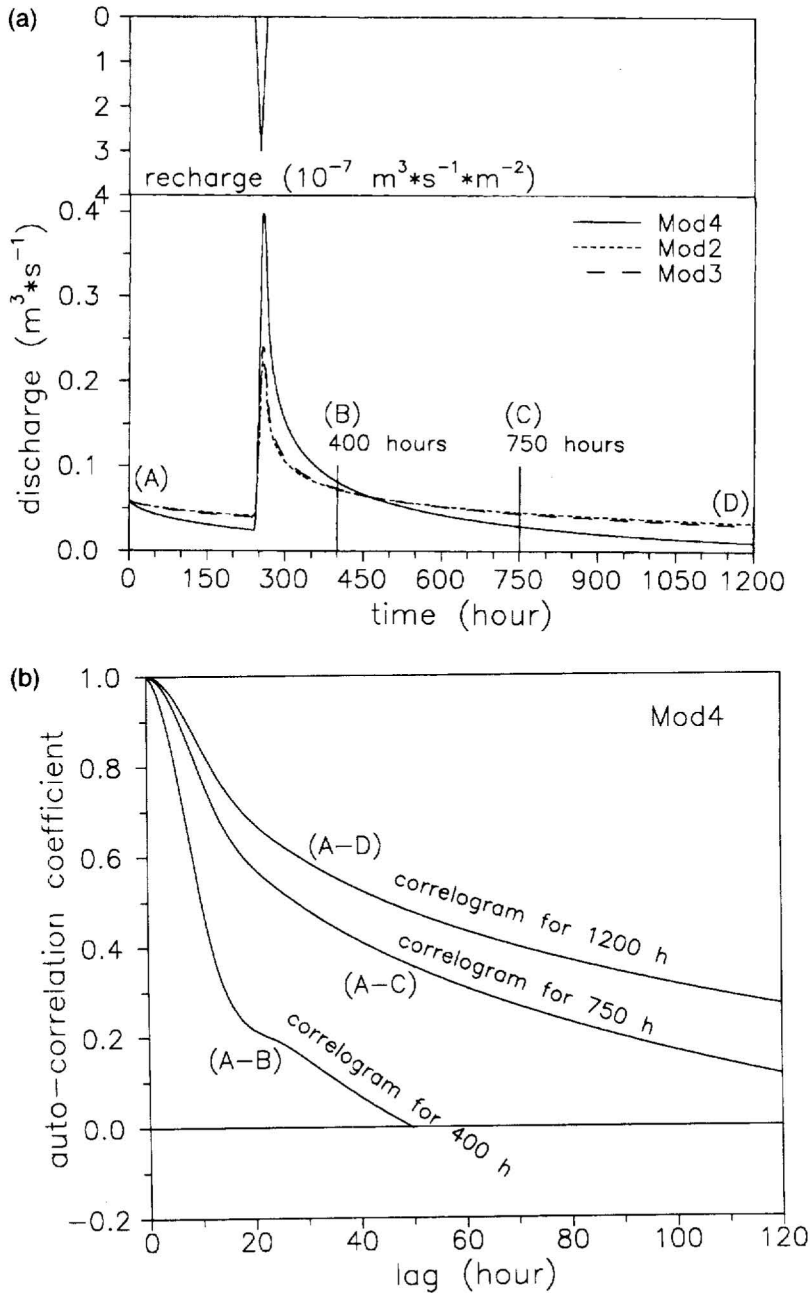

Fig. 6. Spring discharge for the same triangular storm of the models Mod2, Mod3, and Mod4. For letters, see text and Fig. 6(b). (b) Auto-correlation (discharge–discharge) for simulated hydrograph Mod4 for three time periods (see Fig. 6(a), discharge record stopped at 400 hr (A–B), 700 hr (A–C) and 1200 hr (A–D)), m = 130, 230 and 400, respectively.

reserves of Mod4 are smaller than Mod2 and Mod3. (Note that in these different models, the values of K and S_s are identical. The same is also the case for the infiltration rate, directly drained by the karst network).

In order to analyse the influence of base flow discharge on the form of the correlogram, we have studied the simulated hydrograph from Mod4 for three different time intervals chosen randomly (Fig. 6(a)). These intervals are respectively 400 hr of simulation (length A-B), 750 hr (length A-C) and 1200 hr (length A-D). Fig. 6(b) shows the correlograms which correspond to these three intervals. The more or less rapid drop in the auto-correlation function is linked to the length of the recession period analysed. The bigger the length of the base flow considered, the slower the fall of the autocorrelation function. We achieve $r_k = 0.2$ after $k = 1$ day for the segment analysed (A-B) and $k = 6.5$ days for segment (A-D). The length of the base flow will principally depend on the frequency of the flood peaks present in the series analysed and then, on the frequency of rainfall events.

Let us consider the statistical explanation once more. The traditional interpretation of the correlograms of Fig. 6(b) shows two important, different hydrogeological behaviours. The correlogram (A-B) drops sharply, a characteristic of an aquifer with a well developed karst network and small ground water flow reserves. Correlograms (A-C) and (A-D) show a gentle drop in the auto-correlation function, a characteristic of small karstified aquifers with high ground water flow reserves. These interpretations show that for the same karst aquifer, i.e. drainage structure and ground water flow reserves, the shape of the correlogram can give varied information according to the frequency of hydrological events.

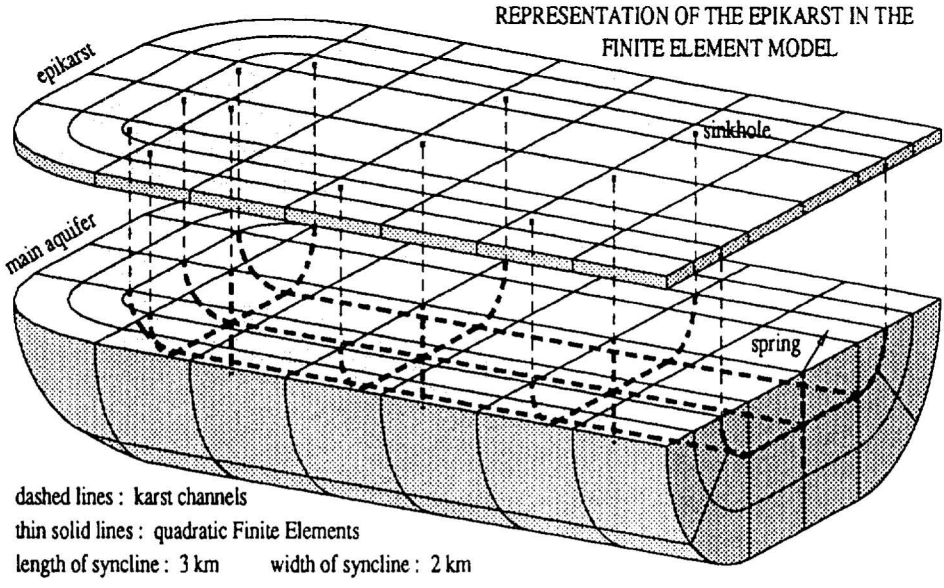

Fig. 7. Finite element network for the variant Mod1. The thin lines represent the boundaries of quadratic finite elements. The thickness of the theoretical aquifer is 50 m.

The analysis highlights that it is not only the quick flow-base flow contrast (see Areuse-Serrière example) that influences the correlogram but also the length of base flow considered in other words, the frequency of hydrological events. This last factor depends on the global configuration of the whole karst aquifer and on rainfall events. As the correlogram depends on the events represented in the record, the rise of floods and their amplitudes will also change it, but less so (Eisenlohr, 1995).

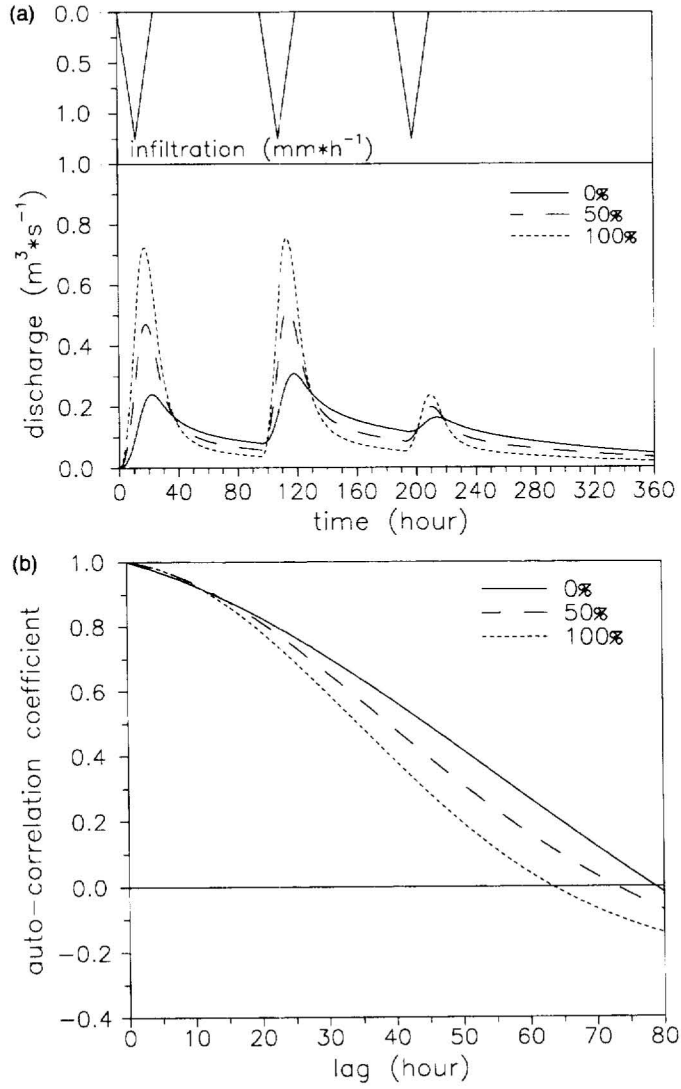

Fig. 8. (a) Mod1 simulated spring discharge for different proportions of infiltration directly drained into the Karst channel network (after Király et al., 1995). (b) Auto-correlation (discharge–discharge) for the simulated floods of Mod1, m = 80. (c) Auto-correlation (discharge–discharge) for the simulated hydrographs of Mod 1, m = 130.

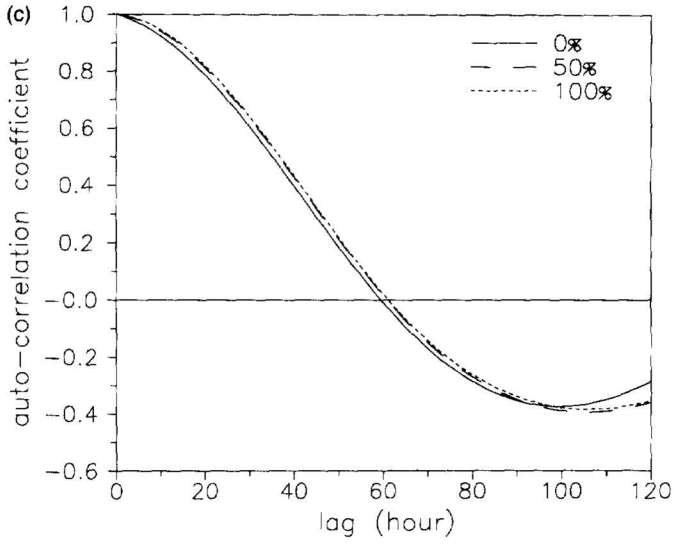

Fig. 8 (*continued*)

5.2. *3-D Numerical simulation of discharge evolution*

Using a 3-D model, we show another key factor for the form of a hydrograph, and, thus a priori for the form of a correlogram. A 3-D model was used (Király et al., 1995) capable of distributing the infiltration of the main aquifer in a variable manner (from 100% diffuse infiltration to 100% concentrated). This theoretical karstic syncline is drained by a network ending at a spring, which is a unique output (Table 2, Fig. 7). Fig. 8(a) depicts the intensity of the infiltrations for three input events, of a duration of 24 hr each. During the first and second event the infiltrations are distributed over the whole syncline. During the third event, infiltration takes place only on a small stripe in the middle part of the model, representing about 30% of the total infiltration area. The volume of the total infiltrations remains the same in each variant, but the proportion of the diffuse and concentrated infiltrations will change from one variant to another. Fig. 8(a) presents three simulated hydrographs for the spring for different infiltration rates drained directly by the karst network. Obviously, the simulated hydrographs are different, notably in their extreme discharges. Analyzing the floods individually, Fig. 8(b) shows that the mode of infiltration also influences the form of the correlogram. The auto-correlation functions reach $r_k = 0.2$ after 49 hr for 100% concentrated infiltration, after 57 hr for 50% and after 65 hr for 0% concentrated infiltration directly drained by the karst network. Note that the drainage structure is the same for the three simulated hydrographs. This example also shows that the size of the ground water flow reserves does not depend solely on the degree of karstification of the aquifer, i.e. its drainage structure, but also on the mode of infiltration. In the fractured limestone volumes of the 3-D model, the karst ground water levels in a recession period are clearly higher when the infiltration is 100% diffuse. Nevertheless, with 100% concentrated infiltration, the karst network can recharge the volumes of rock

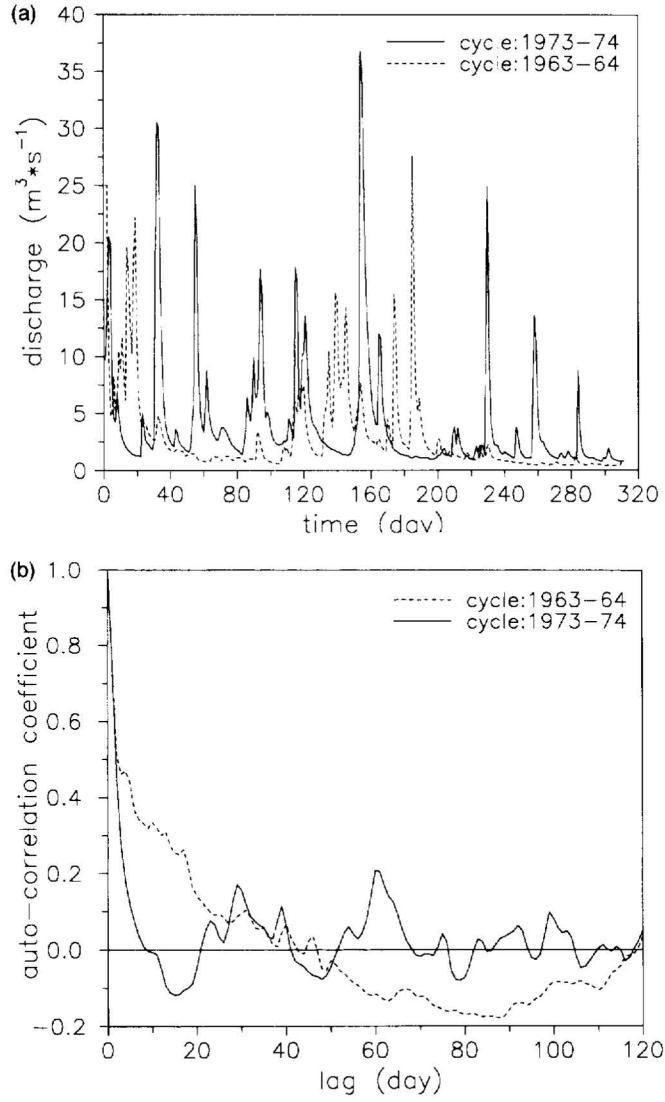

Fig. 9. (a) Hydrographs for the Areuse Spring (———, hydrological cycle 1973–1974; - - -, hydrological cycle 1963–1964). The average daily dischrges are obtained from the federal limnimetric stations (canton of Neuchâtel, Switzerland). Daily rainfall for the same period at the climatic station of Ponts-de-Martels (canton of Neuchâtel). (b) Auto-correlations (discharge–discharge) of the Areuse Spring (———, hydrological cycle 1973–1974; - - -, hydrological cycle 1963–1964), $m = 120$.

with a weak hydraulic conductivity throughout periods of high waters. This inversion of the gradient between the karst network and the low hydraulic conductivity zones changes the state of the ground water flow reserves of the aquifer.

Fig. 8(c) shows the correlograms over the whole simulation period. (i.e. nearly 400 hr).

Fig. 8(c) shows that the discharge–discharge correlograms for these three different simulated hydrographs (0, 50, and 100% of concentrated recharge) have similar behaviour. We explain this result as being due to a very high frequency of flood for the duration of the simulation. The information given by the correlogram can be strongly modified by a high frequency of floods.

We come back to the example of a real aquifer to show that the frequency of flood has an effect on the form of the correlogram that we cannot ignore. Two hydrological cycles (1963–1964 and 1973–1974) of the Areuse Spring have been analysed (Fig. 9(a)). The frequency of hydrological events is higher for the 1973–1974 cycle than for 1963–1964. The discharge–discharge correlograms are given in Fig. 9(b). The auto-correlation function of the 1973–1974 cycle reaches $r_k = 0.2$ after 3.5 days and after 18.5 days for the 1963–1964 cycle that has the lowest flood frequency. This figure clearly shows that for the same karst aquifer, the higher the frequency of the flood, the faster the fall off of the correlogram.

5.3. 2-D Numerical simulation of discharge evolution

We have shown using 2-D and 3-D models the influence of several parameters on the form of the hydrographs and thus on the correlograms. The sensitivity of statistical interpretation (discharge–discharge and precipitation–discharge) was undertaken by simulating hydrographs over several years. A daily recharge over five years 1984–1989 (Bultot et al., 1992) was injected to theoretical karst basins Mod2 and Mod4 (Table 1, Figs. 3 and 4). The hydraulic parameters introduced in the models, K and S_s, and the infiltration mode are identical for Mod2 and Mod4.

Fig. 10(a) depicts two simulated hydrographs for 1985 only. The hydrographs differ in the amplitude of the flood but equally in the values of the discharges in recession period. The flood frequency is the same for both hydrographs. The differences in the simulated hydrograms are only due to the karst network density. The low hydraulic conductivity surfaces are 1000 m^2 and 250 m^2 for Mod2 and Mod4 respectively.

Let us now examine the interpretation of these simulated hydrographs using statistical explanation. Fig. 10(b) shows that the auto-correlation function of Mod4 drops faster than that of Mod2. The correlogram for Mod4 reaches $r_k = 0.2$ after 16 days, whilst for Mod2, it takes 30 days. The statistical interpretation shows that Mod4 has a larger karstic network and lower ground water flow reserves than Mod2. In this case, the statistical interpretation fits with the hydrogeological parameters used in the models presented. The same results have been obtained for the cross-correlation (recharge–discharge, Fig. 10(c)).

6. Summary and conclusion

The first results of the 2-D and 3-D numerical simulations of the theoretical karst basins show that the hydrogeological interpretations made from statistical analysis do not solely depend on the drainage density of the karst network and therefore, the size of the ground water flow reserves. In other words, the relationships correlogram form—degree of karstification of the aquifer—regulatory capacity, are not always correctly deduced. In spite of the limitations inherent in the 2-D and 3-D models, the simulations clearly show

the need for good hydrogeological information about an karst aquifer before using statistical methods. The climatic regime—storm frequency and spatial and temporal distribution of rainfall, the particular infiltration mechanisms of karst, meaning the ratio between diffuse and concentrated infiltration have a major influence on the form of the hydrograph and the correlogram. Without sufficient hydrogeological knowledge we find it

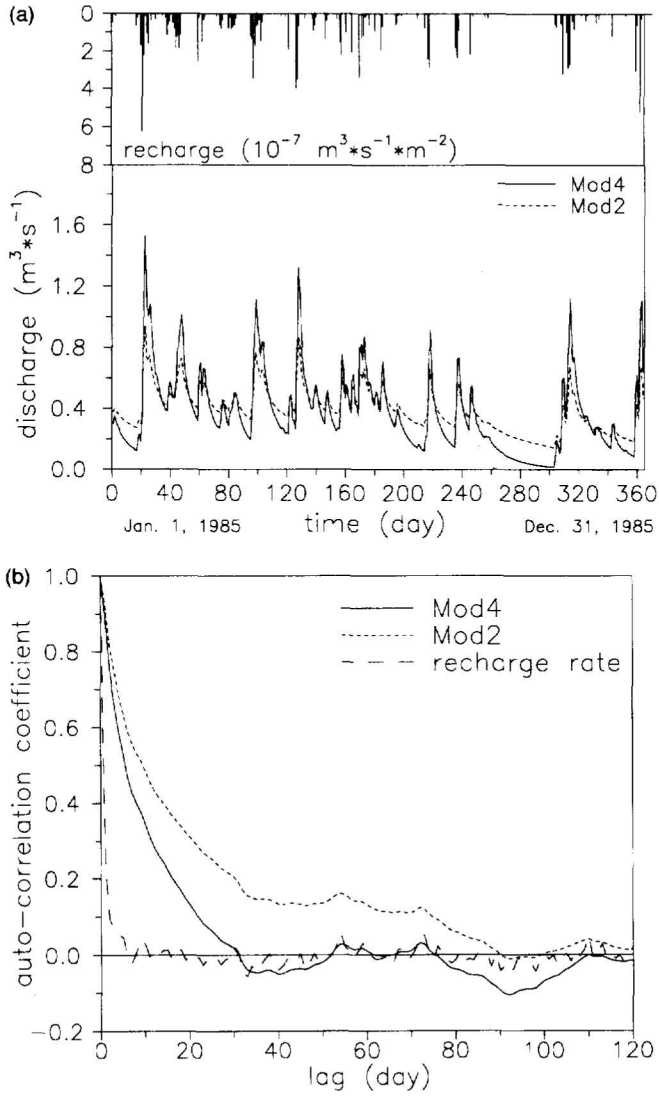

Fig. 10. (a) Spring discharge simulated for the variants Mod2 and Mod4 over a recharge rate of 5 years. The recharge record is taken from Bultot et al. (1992). The figure shows only part of the simulated hydrograph. (b) Auto-correlation (discharge–discharge) for hydrographs of variants Mod2 and Mod4, $m = 600$. (c) Cross-correlation (recharge–discharge) for the hydrographs of variant Mod2 and Mod4, $m = 600$.

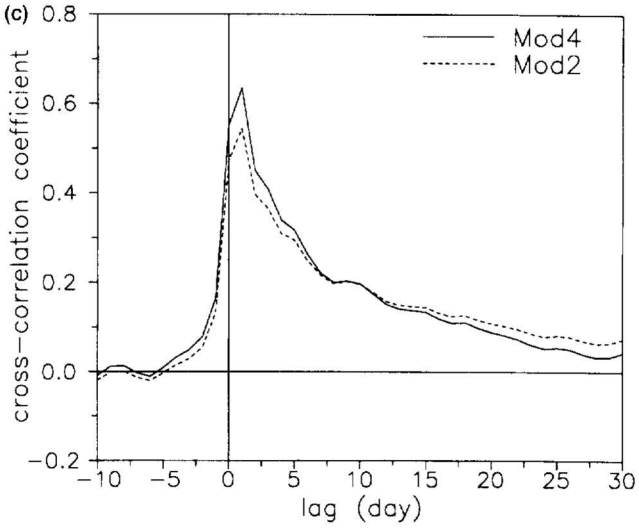

Fig. 10 (*continued*)

difficult to blindly accept comparative results between very different karst aquifers from differing climatic regimes. This knowledge can come from analysis of spring response variability. For example, White (1988) takes into account some exceptional points of the hydrograph to characterize a karst aquifer: a measure of the 'flashiness' of the response is given by the ratio of peak to base flow, Q_{max}/Q_{base} flow, for individual storms or for the annual peak discharge. Several time parameters can be extracted. The lag time, t_L, is the length of time between the storm pulse and the peak in the discharge hydrograph, and the time for return to base flow is t_B. Bonacci (1987, 1993) combined natural and forced responses (discharge from karst springs and hydrodynamic characteristics from wells) to derive some information.

Otherwise, the numerical simulation results we present show that cross-correlation can serve as characteristic operator for the precipitation–discharge relationship. The advantage of the method is that from a rectangular input (one mainly used daily precipitation) we have a reasonable form to the relationship between precipitation and discharge.

Finally, these statistical methods (including decomposition of the hydrographs) are acceptable and reccomended if we wish to predict characteristic discharges, to show trends or even global water resource management; but, we must be careful if we want to get structural and hydrodynamic characteristics of karstic aquifers. The limit of these statistical interpretations is principally linked to the fact that the global response of the karst system is a function of a multitude of variables which make the interpretation problematic.

Acknowledgements

The authors are grateful to O. Bonacci and M. Dzikowsky for their valuable and constructive comments.

References

Atkinsson, T. C., 1977. Diffuse flow and conduit flow in limestone terrain in the Mendip Hills, Somerset (Great Britain), J. Hydrol., 35, 93–103.

Bear, J., 1979. Hydraulics of Groundwater. McGraw-Hill, London, 569 pp.

Bonacci, O., 1987. Karst Hydrology. Springer-Verlag, Berlin, 173 pp.

Bonacci, O., 1993. Karst springs hydrographs as indicators of karst aquifers, J. Hydrol. Sciences, 38 (1–2), 187–198.

Box, G. E. P., Jenkins, G. M., 1974. Time series analysis: forecasting and control. Holden-Day, California, San Francisco, 575 pp.

Brown, M. C., 1973. Mass balance and spectral analysis applied to karst hydrology networks, Water Resour. Res., 9 (3), 749–752.

Bultot, F., Gellens, D., Spreafico, M., Schadler, B., 1992. Repercussions of CO_2 doubling on the water balance—a case study in Switzerland, J. Hydrol., 137, 199–208.

Burger, A., 1992. Hydrogéologie du bassin de la source de l'Areuse. In: Paloc, H., Back, W. (Eds), Hydrogeology of Selected Karst Regions, IAH, Vol. 13, pp. 159–177.

Dreiss, S. J., 1982. Linear kernels for karst aquifers, Water Resour. Res., 18 (4), 865–876.

Drogue, C., 1972. Analyse statistique des hydrogrammes de décrues des sources karstiques, J. Hydrol., 15, 49–68.

Eisenlohr, L., 1995. Variabilité des réponses naturelles des aquifères karstiques: De l'identification de la réponse globale vers la connaissance de la structure de l'aquifère. Thèse Doc. ès Sci., Uni. Neuchâtel, 123 pp.

Eisenlohr, L., Király, L., Bouzelboudjen, M., Rossier, Y., 1997. Numerical simulation as a tool for checking the interpretation of karst spring hydrographs. J. Hydrol. 193 (1–4), 306–315.

Ford D.C., Williams P.W. 1989. Karst Geomorphology and Hydrology. Unwin Hyman, Boston, MA, 601 pp.

Forkasiewicz, J., Paloc, H., 1967. Le régime de tarissement de la Foux de la Vis, Chronique Hydrogéol., Bull. BRGM, 10, 59–73.

Irons, B. M., 1970. A frontal solution program for finite element analysis, Int. J. Num. Math. Eng., 2, 5–32.

Jakeman, A. J., Greenaway, M. A., Jennings, J. N., 1984. Time-series models for the prediction of stream flow in karst drainage systems, J. Hydrol., 23 (1), 21–33.

Király, L., 1973. Notice explicative de la carte hydrogéologique du Canton de Neuchâtel. Centre d'Hydrogéologie Neuchâtel. Bull. Société neuchâteloise Sci. nat., 15 pp.

Király, L., 1975. Rapport sur l'état actuel des connaissances dans le domaine des caractères physiques des roches karstiques. In: Burger, A., Dubertret, L. (Eds.), Hydrogeology of Karst Terrains, Union of Geol. Sci., Vol. B3, pp. 53–67.

Király, L., 1985. FEM 301: A three dimensional model for groundwater flow simulation. NAGRA Technical Report 84–49, Baden, Switzerland, 96 pp.

Király, L., 1988. Large scale 3-D groundwater flow modelling in highly heterogeneous geologic medium. Groundwater flow quality modelling. In: Custodio, E., et al. (Eds), Reidel Publishing Company, Vol. 224, pp. 761–775.

Király, L., Morel, G., 1976. Remarques sur l'hydrogramme des sources karstiques simulées par modèles mathématiques, Bull. Centre Hydrogéol. Neuchâtel, 1, 37–60.

Király, L., Perrochet, P., Rossier, Y., 1995. Effect of the epikarst on hydrograph of karst springs: a numerical approach, Bull. Centre Hydrogéol. Neuchâtel, 14, 199–220.

Knisel, W.G., 1972. Response of karst aquifers to recharge. Hydrol. pap. Colo. state Univ., Fort Collins, Colo., 60, 48 pp.

Kresic, N.A. 1993. Review and selected bibliography on quantitative definition of karst hydrogeological systems. In: Lamoreaux, P. E. (Ed.), Annotated Bibliography of Karst Terrains, Vol. 14, pp. 51–87.

Mangin, A., 1975. Contribution à l'étude hydrodynamique des aquifères karstiques. Thèse Doc. ès Sci., Annales Spéléo., 29, 285–382; 495–601; 30, 21–124.

Mangin, A., 1984. Pour une meilleure connaissance des systèmes hydrologiques à partir des analyses corrélatoire et spectrale, J. Hydrol., 67, 25–34.

de Marsily, G., 1986. Quantitative hydrogeology. Groundwater Hydrology for Engineers. Academic Press Inc., London, 275 pp.

Mathey, B., 1976. Hydrogéologie des bassins de la Serrière et du Seyon. Thèse Doc. ès Sci., Uni. Neuchâtel, 325 pp.

O.E.C.D., 1988. The international HYDROCOIN Project. Level 1: code verification. OECD Publications, Paris, 198 pp.

Ozis, U., Keloglu, N. 1976. Some features of mathematical analysis of karst runoff. In: Yvevjevich, V. (Ed.), Karst Hydrology and Water Resources, Colorado. Water Resource Publications, Vol. 1, pp. 221–35.

Padilla, A., Pulido-Bosch, A., Mangin, A., 1994. Relative importance of baseflow and quickflow from hydrographes of karst spring, Ground Water, 32 (2), 267–277.

Padilla, A., Pulido-Bosch, A., 1995. Study of hydrographs of karstic aquifers by means of correlation and cross-spectral analysis, J. Hydrol., 168, 73–89.

Schoeller, H., 1967. Hydrodynamique dans le karst, Chronique Hydrogéol., BRGM, 10, 7–21.

Soulios, G., 1991. Contribution à l'étude des courbes de récession des sources karstiques: exemples du pays Hellenique, J. Hydrol., 127, 29–42.

Tripet, J.P., 1973. Etude hydrogéologique du bassin de l'Areuse (Jura neuchâtelois). Thèse Doc. ès Sci., Uni. Neuchâtel, 183 pp.

White, W.B., 1988. Geomorphology and Hydrology of Carbonate Terrain. Oxford University Press, Oxford, 464 pp.